Isoleucine Epimerization for Dating Marine Sediments: Importance of Analyzing Monospecific Foraminiferal Samples

Abstract. *The rate of isoleucine epimerization in fossil planktonic foraminifera is strongly species-dependent. Alloisoleucine/isoleucine ratios of two species of the same age can vary by more than a factor of 2. This finding, in combination with the known temporal and spatial variability of foraminiferal assemblages, demonstrates the critical importance of basing geochronological studies of marine sediments on monospecific samples. One rapidly epimerizing species generates a calibration curve of potentially high precision for dating sediments between the ages of about 50,000 to 400,000 years.*

Isoleucine epimerization (*1*) was first proposed 8 years ago as a potentially useful reaction for dating calcareous marine sediments (*2*). This suggestion followed the discovery of a nonprotein amino acid, D-alloisoleucine, in fossil shells and the accompanying observation that the ratio of D-alloisoleucine to L-isoleucine increases in progressively older samples (*3, 4*). Although subsequent research on deep-sea sediments has established the general trend of an increasing D-alloisoleucine to L-isoleucine ratio with age (*5–10*), efforts to develop an accurate, precise dating technique have been largely unsuccessful. A major obstacle to both theoretical and empirical approaches has been the critical need for an amino acid–containing sedimentary component that could be used with confidence as a reliable sampling basis for the technique. We present evidence in this report indicating that a monospecific sample of planktonic foraminifera is such a basis for accurately measuring the rate of isoleucine epimerization in calcareous deep-sea sediments.

Although some of the earlier investigations were based on the analysis of bulk (total) sediment (*5, 6*), the advantages of the foraminiferal fraction soon became apparent. The enclosing calcite skeletons of planktonic foraminifera tend to protect the internal organic matrix from bacterial and physicochemical attack as well as shield the matrix from possible in situ contamination (*7, 11*).

The first detailed foraminifera-based study of isoleucine epimerization was conducted by Wehmiller and Hare (*7*), who used the sediment coarse fraction (>74 μm). This fraction of a well-preserved, highly calcareous deep-sea core consists mainly of a mixed assemblage of planktonic foraminiferal species. Their results suggested that the epimerization reaction consists of two phases: (i) an initial, linear (*12*) phase of rapid epimerization (~0 to 400,000 years), and (ii) a subsequent nonlinear phase of substantially slower epimerization (~400,000 to 2.2 million years). These rates were confirmed by Bada and Schroeder (*8*) with kinetic studies at elevated temperatures.

As a result of finding marked species-specific variations in both amino acid composition and concentration among fossil planktonic foraminifera (*11, 13*), a study was made by King and Hare (*9*) to measure the epimerization rates of individual species. Also, monogeneric studies of isoleucine epimerization in fossil bivalve *Mercenaria* had demonstrated the value of minimizing species effects (*14*). Monospecific samples from selected horizons (0.7 to 1.86 million years) of well-dated cores showed striking differences in the extent of epimerization with the maximum values exceeding the minimum by a factor of nearly 2. In contrast to the nonlinear curve of the polyspecific samples (*7*), the epimerization curves of the individual species proved to be a family of straight lines having essentially the same slope but different intercepts. The observed slow epimerization rate can be advantageously used as a basis for estimating the ages of sediments back to the Middle Miocene (*9*).

Although no data were collected by King and Hare (*9*) for monospecific samples younger than 700,000 years, the positions of the species curves for the older samples on their plot dictate upper segments of accelerated rates analogous to the 0 to 400,000-year segment of the mixed species plot of Wehmiller and Hare (*7*). Because of the potentially steep slopes of the younger segments and resulting high precision for dating purposes, the present study was initiated to detail possible species effects in the interval of 0 to 700,000 years.

The equatorial Pacific deep-sea core V28-238 (0°01′N, 160°29′E) was selected for this study because of an unusual combination of favorable attributes. This highly calcareous core represents a continuous record of well-preserved, undisturbed sediments for which a detailed oxygen isotope stratigraphy has been developed within a paleomagnetic framework (*15*). Moreover, variation in bottom water temperature, a potentially complicating factor in down-core epimerization studies (*7*), can reasonably be assumed to have been well under 1°C over the past 700,000 years (*16*).

Two species of planktonic foraminifera, *Globigerinoides sacculifer* (spinose) and *Globorotalia tumida* (nonspinose), were each isolated from samples taken at 100-cm intervals from the top of V28-238 through the 1200-cm level. Since a magnetic reversal occurring at 1200 cm was identified as the Brunhes/Matuyama boundary (*15*), the oldest sample (1200 cm) analyzed had an age of 700,000 years (*17*). The selection of these two species was based on a number of factors: (i) their taxonomic dissimilarity at the family level based on shell structure (spinose Globigerinidae and nonspinose Globorotaliidae) (*18*) and amino acid composition (*11, 13*), (ii) the marked difference in epimerization rates previously observed between the spinose *Globigerinoides conglobatus* (closely related to *G. sacculifer*) and the nonspinose *Globorotalia crassaformis* (closely related to *G. tumida*) (*9*), (iii) their widely differing susceptibilities to dissolution (*19*), and (iv) their common occurrence and high abundance in calcareous marine sediments. We selected these widely dissimilar species with the objective of defining, as closely as possible, the maximum range of species effects.

Samples (2 to 3 mg of skeletal material) were prepared and the resulting hydrolyzates analyzed in duplicate with a Durrum D-500 amino acid analyzer in accordance with previously reported procedures (*11, 13*).

Measured concentrations of alloisoleucine (A) and isoleucine (I) in duplicate analyses were used to calculate the $(X_e - X)/X_e$ values listed in Table 1 and plotted in Fig. 1. This approach, originally described by Wehmiller and Hare (*7*), measures the degree of epimerization as a fraction of the completed reaction. The expression X_e is the value of A/(A + I) at equilibrium and X is the value of the same ratio at time t. The X_e value used in the present study was 0.583, which is equivalent to an equilibrium A/I ratio of 1.40 (*20*). An equivalent expression of $(X_e - X)/X_e$ is $[1 - 0.715(A/I)]/[1 + (A/I)]$.

The time scale shown in Fig. 1 is the interpolated scale used for V28-238 by Shackleton and Opdyke (*15*). It is based on an assumed uniform sedimentation rate of 1.71 cm per 1000 years and is calibrated by the occurrence at 1200 cm of the Brunhes/Matuyama magnetic boundary of age 700,000 years.

The most striking feature of the species curves plotted in Fig. 1 is the immediate divergence in epimerization curves below the sediment-water interface. The

Table 1. Epimerization of isoleucine in two species of planktonic foraminifera (*Globigerinoides sacculifer* and *Globorotalia tumida*) isolated from deep-sea core V28-238. Concentrations of D-alloisoleucine (allo-Ile) and L-isoleucine (Ile) are expressed in nanomoles per gram of skeletal material. All values are based on duplicate analyses. S.D., standard deviation.

Depth in core (cm)	*Globigerinoides sacculifer*					*Globorotalia tumida*				
	allo-Ile (A)	Ile (I)	A/I	$(X_e - X)/X_e$		allo-Ile (A)	Ile (I)	A/I	$(X_e - X)/X_e$	
				$\bar{X}$	S.D.				$\bar{X}$	S.D.
0	2.5	97.0	0.026	0.958	0.001	1.7	80.0	0.021	0.964	0.003
100	6.1	96.9	.063	.899	.005	7.9	75.9	.104	.840	.001
200	9.4	81.5	.115	.823	.004	14.0	67.6	.207	.706	.011
300	12.1	70.0	.173	.747	.008	15.0	48.2	.311	.593	.004
400	14.5	76.1	.191	.727	.006	20.4	54.6	.374	.535	.004
500	16.1	83.4	.193	.723	.002	23.2	54.7	.424	.489	.007
600	16.4	78.8	.208	.705	.017	20.8	43.0	.484	.439	.003
660	20.6	77.5	.266	.641	.001					
700	20.3	67.5	.301	.603	.013	24.4	46.2	.528	.408	.001
800	20.3	65.0	.312	.593	.011	28.8	51.4	.560	.385	.001
900*						24.3	45.5	.534	.403	.011
1000	20.9	63.1	.331	.574	.017	28.6	50.9	.562	.383	.005
1100	24.3	69.2	.351	.554	.004	27.9	48.0	.581	.369	.007
1200	24.7	64.7	.382	.527	.012	31.7	54.7	.580	.372	.006

*Analysis of *G. sacculifer* was precluded by its extremely low abundance at this level.

degree of divergence then changes with depth (time) until 700 cm (~400,000 years) at which point the difference remains nearly constant through the oldest sampled level (700,000 years). This subparallelism between species curves was originally observed with older (0.7 to 1.86 million years) samples of single species (*9*).

As shown in Fig. 1, the analytical data for each species can be represented by a series of connected straight line segments. The epimerization curve for *Globigerinoides sacculifer* appears to be composed of four segments, one more than exhibited by *Globorotalia tumida*. Inflection points for both species occur at 300 cm (~170,000 years) and 700 cm (~400,000 years) with *G. sacculifer* displaying an extra one at 600 cm. The presence of the extra segment (600 to 700 cm) in the *G. sacculifer* curve has been confirmed by analyzing an intermediate (660 cm) sample. The $(X_e - X)/X_e$ value for this point falls on the line connecting the 600 and 700 cm values.

The underlying reasons for the marked differences in the species curves are not known. Although two possible mechanisms for epimerization in polyspecific samples have been proposed in general terms (*7, 8*), a definitive epimerization model must explain these observed interspecific variations in terms of species-characteristic parameters, for example skeletal ultrastructure or protein composition.

The value of these empirical curves for dating deep-sea sediments with acceptable precision is a function of the steepness of their slopes. Accordingly, the upper two segments (0 to 170,000 and 170,000 to 400,000 years) of the *G. tumida* curve (Fig. 1) are particularly promising for this application. Based on the maximum variability (standard deviation = ±0.011) encountered among duplicate analyses for *G. tumida* in V28-238 (Table 1), the potential precision of this technique is about ±5000 years in the first (0 to 170,000 years) segment and approximately ±15,000 years in the second (170,000 to 400,000 years) segment. It should be emphasized that the actual precision of this calibration curve is dependent on the time scale used for calibration. For example, Shackleton and Opdyke (*15*) considered ±20,000 to be a minimum uncertainty for the 400,000 year level in V28-238.

For dating purposes, the minimum useful age limit for the *G. tumida* curve is about 50,000 years because of the difficulty in accurately measuring the low levels of D-alloisoleucine found in younger samples. The maximum age limit for reasonably high-precision dating is 400,000 years because of the sharply reduced epimerization rates of older samples.

We interpret the mixed species data of Wehmiller and Hare (*7*) to represent average epimerization values controlled primarily by the epimerization rate and relative abundance of each individual species in the foraminiferal fraction. It is widely recognized that the faunal assemblage of foraminiferal species in deep-sea sediments varies temporally and spatially in response to climate (*21*) and carbonate dissolution intensity (*22*). As a specific example, the relative percentages of *G. sacculifer* and *G. tumida* vary from 9 to 22 percent and from 0 to 11 percent (*21*), respectively, in the sampled levels of one of the key cores (V12-122) of Wehmiller and Hare (*7, 23*). Thus, the scatter in the average epimerization values for mixed species [(*7*) and Fig. 1, inset] can be explained in terms of the different species rates acting through a changing faunal assemblage. It is interesting to note that, with the exception of two young (<50,000 years) samples, fluctuations in the mixed species values are delimited by the two species curves (Fig. 1, inset).

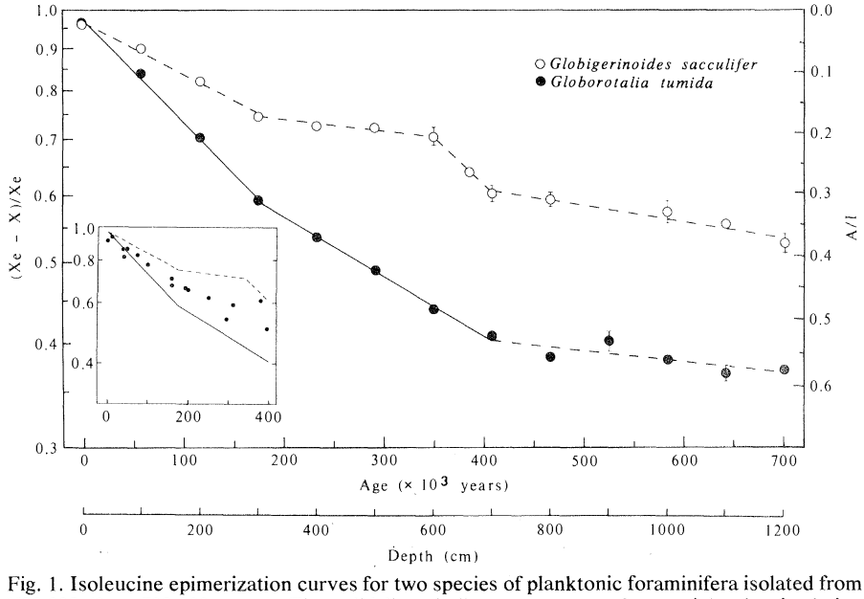

Fig. 1. Isoleucine epimerization curves for two species of planktonic foraminifera isolated from V28-238 (0 to 700,000 years). The solid lines indicate segments of potential value in dating marine sediments ~50,000 to 400,000 years old. Symbols (circles) enclose the standard deviations of duplicate analyses, except where noted by uncertainty bars. Each line segment was generated by a least-squares fit. The inset shows the mixed species data (0 to 400,000 years) of Wehmiller and Hare (*7*) plotted with the species curves. $(X_e - X)/X_e$ is equivalent to $[1 - 0.715(A/I)]/[1 + (A/I)]$.

In summary, the two species curves developed in this study (Fig. 1) clearly demonstrate the advantages of monospecific samples for: (i) eliminating the errors (scatter) generated by the variability in foraminiferal assemblages, and (ii) providing a high degree of dating precision through rapidly epimerizing species, for example *G. tumida* (50,000 to 400,000 year range). If intercore correlations now being studied are successful, the *G. tumida* curve for V28-238 (Fig. 1) could be used as an empirical calibration curve for dating marine sediments at any location. Species curves, with their minimal scatter and linear segmented nature, provide a promising basis for future empirical and modeling studies of isoleucine epimerization in deep-sea sediments.

KENNETH KING, JR.
COLLEEN NEVILLE
Lamont-Doherty Geological Observatory of Columbia University, Palisades, New York 10964

References and Notes

1. The term epimerization is used in this report, rather than racemization, to describe the configurational change from L-isoleucine to D-alloisoleucine. Epimerization is the preferred term for conversions involving compounds, such as isoleucine, with two asymmetric carbon atoms.
2. P. E. Hare and R. M. Mitterer, *Carnegie Inst. Washington Yearb.* **67**, 205 (1969).
3. ———, *ibid.* **65**, 362 (1967).
4. P. E. Hare and P. H. Abelson, *ibid.* **66**, 526 (1968).
5. K. A. Kvenvolden, E. Peterson, F. S. Brown, *Science* **169**, 1079 (1970).
6. J. L. Bada, B. P. Luyendyk, J. B. Maynard, *ibid.* **170**, 730 (1970).
7. J. Wehmiller and P. E. Hare, *ibid.* **173**, 907 (1971).
8. J. L. Bada and R. A. Schroeder, *Earth Planet. Sci. Lett.* **15**, 1 (1972).
9. K. King, Jr., and P. E. Hare, *Carnegie Inst. Washington Yearb.* **71**, 596 (1972).
10. K. A. Kvenvolden, E. Peterson, J. Wehmiller, P. E. Hare, *Geochim. Cosmochim. Acta* **37**, 2215 (1973).
11. K. King, Jr., and P. E. Hare, *Science* **175**, 1461 (1972).
12. Data on isoleucine epimerization in marine sediments have been largely interpreted in terms of a reversible first-order kinetic model. A linear relationship between log $[(X_e - X)/X_e]$ and sediment age indicates a reversible first-order mechanism according to the approach of Wehmiller and Hare (*7*). X_e is the value of alloisoleucine/(alloisoleucine + isoleucine) at equilibrium, and X is the value of this ratio at time t.
13. K. King, Jr., and P. E. Hare, *Micropaleontology* **18**, 285 (1972).
14. R. M. Mitterer, in *Advances in Organic Geochemistry: 1971*, H. R. von Gaertner and H. Wehner, Eds. (Pergamon, Elmsford, N.Y., 1972), p. 441.
15. N. J. Shackleton and N. D. Opdyke, *J. Quat. Res.* **3**, 39 (1973).
16. N. J. Shackleton, personal communication.
17. G. B. Dalrymple, in *Calibration of Hominoid Evolution*, W. W. Bishop and J. A. Miller, Eds. (Scottish Academic Press, Edinburgh, 1972), p. 107.
18. A. W. H. Bé, in *Fiches Ident. Zooplancton*, No. 108 (1967).
19. W. H. Berger, *Deep-Sea Res.* **15**, 31 (1968).
20. This equilibrium alloisoleucine/isoleucine ratio of 1.40 is based on previously reported values for Middle Miocene *Mercenaria* (*3*) and Lower Paleocene planktonic foraminifera (*7*).
21. J. Imbrie and N. G. Kipp, in *Late Cenozoic Glacial Ages*, K. K. Turekian, Ed. (Yale Univ. Press, New Haven, 1971), p. 71.
22. W. H. Berger, *J. Foraminiferal Res.* **3**, 187 (1973).
23. These faunal changes may approximate a minimum response, since this Caribbean core (water depth 2730 m) reflects a relatively narrow range of paleoclimatic variations and a minimal degree of carbonate dissolution (*20*).
24. We thank J. D. Hays, N. D. Opdyke, N. J. Shackleton, and J. F. Wehmiller for their helpful comments on the manuscript. The technical assistance of P. Manley is gratefully acknowledged. Supported by National Science Foundation grants DES72-01571, DES75-18136, IDOE GX 28671, and a Columbia University faculty fellowship to C.N. Contribution No. 2478 of the Lamont-Doherty Geological Observatory.

28 September 1976; revised 30 November 1976

Sunlight-Induced Bromate Formation in Chlorinated Seawater

Abstract. *Chlorinated waters are being introduced into estuarine and coastal areas in increasing quantities. In such systems, the chlorine reacts with the natural bromide and ammonia to produce the highly toxic hypobromous acid, hypobromite ion, and haloamines. Sunlight causes up to 50 percent conversion to bromate ion, which is persistent in natural waters and has an unknown toxicity.*

Chlorine and its compounds have been used for water disinfection and as general aqueous biocides in increasing quantities since the turn of the century. The popularity of these materials stems partly from the remarkable apparent tolerance of mammals to them (*1*) at concentrations that produce mortality of organisms ranging from bacteria to fish; that is, it kills them, not us. Recent estimates (*2*) indicate that more than 100,000 tons of chlorine are used annually for the partial disinfection of effluents from wastewater treatment plants, and such use may be expected to increase substantially as the secondary treatment systems mandated by Congress in Public Law 92–500 begin operation. An additional major use of these compounds is as antifouling agents in the cooling waters of electric generating plants. Somewhat more chlorine is used for this purpose than for wastewater treatment, based on a cooling water flow of 300,000 cubic feet per second (8400 m^3/sec) (*3*) and a dose of 0.5 mg of Cl_2 per liter.

The release of chlorinated waters is producing effects that are slowly being better documented as a result of continuing research. Summaries of current knowledge (*4*) show avoidance behavior and reproductive failure in many freshwater invertebrates and fish at chlorine concentrations of 0.003 to 0.005 mg/liter. Federal and state regulations have been based on measurements of "residual chlorine" for both control of wastewater treatment (in the state of Virginia, chlorine is added until the concentration in effluent is 2.0 mg/liter) and effluent limitations on power plants. Considering the strong sensitivity of aquatic organisms to "residual chlorine" and the present levels of chlorine use, substantial damage to aquatic resources may occur. For example, the present releases of chlorine to Chesapeake Bay and its tributaries would sterilize the whole system if there were not environmental degradation of the added chlorine. However, transformation of chlorine to persistent, but less acutely toxic, compounds may be hypothesized to produce slow changes in the abundance and diversity of aquatic species in such situations.

Degradation is operationally defined as the disappearance of the analytical signal for "residual chlorine." As pointed out by Eppley *et al.* (*8*), different analytical methods produce very different estimates of "residual chlorine." In fact, the products from chlorination of wastewaters and natural waters are a mixture of chlorine, hypochlorous acid, hypochlorite ion, inorganic and organic chloramines, and other compounds. A better term is "residual oxidants," and we use this in the remainder of this report.

Since a large fraction of the U.S. population resides in coastal areas, much of the chlorine is discharged to saline natural waters. There is an extensive literature (*4*) on chlorination of freshwater systems, but coastal and estuarine waters have not been studied extensively. Research programs are under way at several federal and university marine laboratories to alleviate this situation. The work on freshwaters, unfortunately, does not have much application to marine environments, because seawater has a bromide ion concentration of 65 mg/liter and the added chlorine reacts with it to produce hypobromous acid and hypobromite ion. Bromamines and chloramines may be formed in the presence of ammonium ion (*5*).

For normal seawater of pH 8, the initial products of chlorination are a mixture of hypobromous acid and hypobromite ion. Both of these compounds are unstable with respect to decomposition and disproportionation.

$$2HOBr \rightarrow 2H^+ + 2Br^- + O_2;$$
$$2OBr^- \rightarrow 2Br^- + O_2 \quad (1)$$

$$3HOBr \rightarrow 3H^+ + 2Br^- + BrO_3^-;$$
$$3OBr^- \rightarrow 2Br^- + BrO_3^- \quad (2)$$